J Mar Sci Technol
DOI 10.1007/s00773-014-0275-0

ORIGINAL ARTICLE

Higher order hydrodynamic interaction between two slender bodies in potential flow

Usama Kadri · Daniel Weihs

Received: 2 September 2013 / Accepted: 11 May 2014

Abstract In this paper, we apply the slender body theory to study the effect of higher order hydrodynamic interactions between two slender bodies of revolution moving in close proximity, in an unbounded, inviscid, and incompressible fluid. We compare between leading and second-order approximations, as well as approximate and exact separation distances. The total solution is found to be valid for both small and large lateral separation distances. The contribution of the higher order forces is found to be relatively small for large separation distances, though significant for small separation distances. Comparisons with measurements and simulations are satisfactory.

Keywords Slender body · Hydrodynamic interaction · Higher order effects

1 Introduction

When two submerged bodies move in close proximity, or when a moving body passes a stationary one, interactions involving significant hydrodynamic forces and moments occur. In potential flow, one can show, via the Galilean transformation, that a body moving in still water has equivalent forces to the case of unmoving bodies in a stream of equal and opposite velocity. Assuming potential flow, a particular case of special interest is the steady-state case where two bodies move side by side or in tandem, such as in a refuelling manoeuvre, or when a single body is moving parallel to a wall. Several theoretical and experimental studies [1–6] investigated this problem, mostly concerning ship–to–ship interactions. Most of these previous works were motivated by the operation of replenishment at sea. The "bank–suction" problem (e.g. see [6]) is related, by the method of images, to the refuelling problem for two identical ships directly abeam of each other when the bank is a vertical wall. In each of these various problems, hydrodynamic interaction forces and moments may lead to collision, breakage of mooring lines, or grounding.

The analyses and experiments done by [1–3] were dealt with calculations or measurements of the lateral force and yawing moment on two ship hulls moving at equal velocities, side by side or in tandem, in deep water. For bodies moving at different velocities, [4] developed a two-dimensional theory for elliptical cylinders. Using the same method [5] analysed the manoeuvring problem relevant to collision situations. By taking the slender body theory approach, for the steady-state bank–suction problem, or the equivalent refuelling problem, slender body results have been developed by Newman [7] and [8] for axisymmetric bodies and for slender pointed bodies of an arbitrary cross-section. Reference [9] investigated the hydrodynamic interactions on a moored vessel resulting from a passing ship at various separation distances.

The horizontal translation of slender bodies of revolution near a plane wall was investigated by Newman [7], who gave an explicit solution of the flow in terms of a curved-line source distribution inside the body, and a corresponding image source system below the wall.

Electronic supplementary material The online version of this article (doi:10.1007/s00773-014-0275-0) contains supplementary material, which is available to authorized users.

U. Kadri (✉)
Department of Mechanical Engineering, Massachusetts Institute of Technology, Cambridge, MA 02139, USA
e-mail: usama.kadri@gmail.com

D. Weihs
Faculty of Aerospace Engineering, Technion, Israel Institute of Technology, 32000 Haifa, Israel

Published online: 10 June 2014

Reference [10] has extended the work of Newman [7] to include the effects of the angle of attack and ground undulation. Some general motions of spheres and ellipsoids were investigated by Milne-Thomson [11]: two spheres moving at right angles to the line of centres, a sphere moving perpendicularly to a wall, a sphere moving parallel to a wall, and the motion of ellipsoids. In each of these problems, that involve two bodies, Milne-Thomson [11] assumed a large distance between the two bodies, and each body was almost unaffected by the presence of the other.

While originally slender body theory was introduced into fluid mechanics by Munk [12] for calculating the lift of airships [13–15], and others established related theories of matched asymptotic expansions. Fluid dynamic problems involving slender bodies moving in very close proximity to the ground are of practical importance, among others, in connection with high-speed ground transportation vehicles [16, 17], and with respect to the interaction between a ship hull and an adjacent canal wall or section ship [6, 18]. The applications of slender body theory to ship hydrodynamics are reviewed by Newman [19], and Ogilvie [20, 21]. A survey of ship hydrodynamics in restricted water is given by Tuck [6]. Reference [22] extended Collatz's problem to three-dimensional ship form and presented slender body results of the lateral force and the yawing moment. They considered two slender bodies of arbitrary different forms moving at constant velocities not necessarily equal, and they relaxed the pointed-end condition to allow a low aspect ratio trailing edge effect at the stern. Furthermore, the interaction of slender ships in shallow water and with fixed obstacles were investigated by Yeung [23, 24]; and the interaction between two lifting bodies and two ships in proximity to bank wall has been studied by Kijima [25] and [26], respectively.

Slender body theory has been applied more recently to analyse the flow field near slender bodies with complex geometries (e.g. [27–30]). Some special applications also exist, such as in the case of fish swimming [31, 32], or in the case of dolphin mother–calf interaction which explains the extra gain of thrust by the calf [33]. More recently, Wang [34] studied the hydrodynamic interaction (lateral force and yawing moment) of two slender bodies translating in very close proximity, using matched asymptotic expansions and conformal mapping for the inner solution. The analytical solution by Wang [34] agrees well with the boundary element model (BEM) by Nathman [35], for very small lateral separation distances. However, an increasing deviation from the BEM is observed with increasing the separation distance.

The present work considers the interaction of hydrodynamic longitudinal force between two prolate bodies of revolution moving at constant, though not necessarily equal, velocities and having various separation distances. Empirical evidence and theoretical analyses show that the effect on moving bodies is less than on stationary ones (e.g. [22, 34]). We extend the general solution by Tuck [22] who assumed large lateral separation distance between the two bodies, compared with their lateral dimensions. Thus, each body is considered in the far field of the other, and if the leading order is assumed, the flow fields produced by each body can be computed as if the other was absent. We are interested, among others, in the small separation problem (but still neglecting the boundary layer). Therefore, we consider higher order approximation terms to find the direct forces acting on body 1 due to the movement of body 2, and the higher order forces due to the movement (or presence) of body 1. Note that the free surface effects are neglected in the analysis, since we are interested in the problem of ships in calm water [19, 22], as well as the problem of submerged bodies far from the surface. The latter problem is important, among others, for studying dolphin mother–calf separation in chase situations, which has become a major concern in fishing-related cetacean mortality [33]. It is also relevant for the interaction of a submarine with the seafloor, another submarine, or launched missiles.

The formulation and solution of the general problem are presented in Sect. 2. The second-order solution for the forces acting on the body is considered in Sect. 3, where the exact separation distance is introduced, and the contribution of the neglected viscous effects is discussed.

2 Background

Consider the problem of two prolate bodies of revolution (see Fig. 1) moving in unbounded inviscid and incompressible fluid with

$$d_j/L_j = \epsilon_j \tag{1}$$

where d_j and L_j are the maximum lateral and longitudinal dimensions of the jth body, and the slenderness parameter ϵ_j is assumed to be small for both bodies. On this basis, an approximate solution is sought for the hydrodynamic quantities of interest. The two streamlined bodies move through a potential fluid with constant velocities U_1 and U_2 along parallel paths. The relative positions of the two bodies change in time at a rate allowing a quasi-steady flow approximation (i.e. any instant the flow is considered steady). The two bodies are separated by a constant lateral distance η_0, and fore-and-aft distance ξ, which is a function of time t. Two coordinate systems, (x_1, y_1, z_1) fixed on body 1 and (x_2, y_2, z_2) fixed on body 2 (see Fig. 1), are related to the fixed coordinate system so that

$$\begin{aligned} &x_0 = x_1 + U_1 t = x_2 + U_2 t - \xi(0); \\ &y_0 = y_1 = y_2 + \eta_0; \quad z_0 = z_1 = z_2, \end{aligned} \tag{2}$$

where

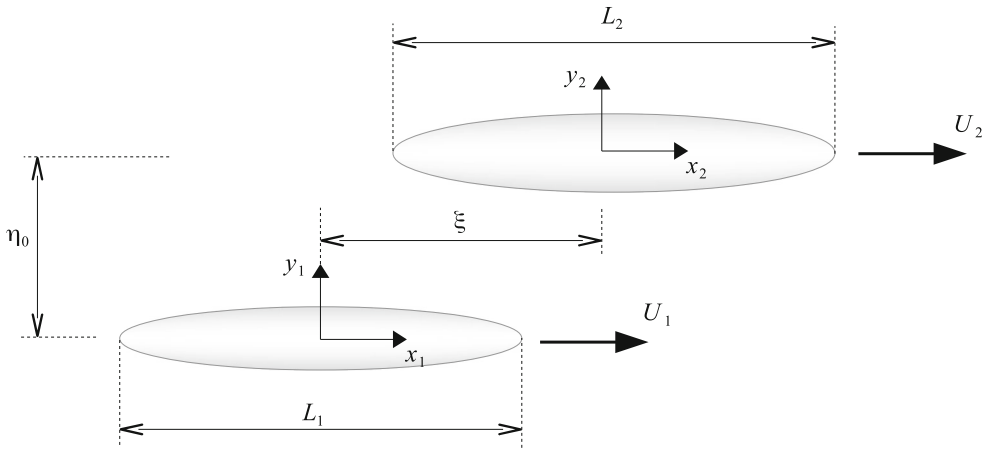

Fig. 1 Two slender bodies of lengths L_1 and L_2 separated by a lateral distance η_0 and a longitudinal distance $\xi(t)$, moving with velocities U_1 and U_2, respectively

$$\xi(t) = x_2 - x_1 = (U_1 - U_2)t + \xi(0). \tag{3}$$

At this stage, we assume that the separation distance η_0 is $O(1)$, large compared to the lateral dimensions of the bodies that is $O(\epsilon)$. For this approximation we calculate the flow field produced by each body as if the other was absent since the lateral separation between the two bodies is large compared to their lateral dimensions and each body is in the other's far field so that it appears as a line with vanishing lateral thickness. Thus, the flow about each body is asymptotically steady, and can be estimated by standard methods of slender body theory for the steady motion of a single body in an infinite fluid [36]. Following [22] the longitudinal and lateral velocity components of the induced stream of body 2, evaluated on the axis of body 1 are

$$U(x_2) = \frac{U_2}{4\pi} \int_{L_2} \frac{S_j'(x)(x_2 - x)\,\mathrm{dx}}{\left[(x_2 - x)^2 + \eta_0^2\right]^{3/2}}, \tag{4}$$

and

$$V(x_2) = \frac{U_2 \eta_0}{4\pi} \int_{L_2} \frac{S_2'(x)\,\mathrm{dx}}{\left[(x_2 - x)^2 + \eta_0^2\right]^{3/2}}. \tag{5}$$

The corresponding longitudinal and lateral forces for a longitudinally symmetric body are

$$X = \frac{\rho U_2^2}{4\pi} \int_{L_1} S_1'(x_1) \int_{L_2} \frac{S_2'(x_2)(x_2 - x_1 - \xi)\,\mathrm{dx_2\,dx_1}}{\left[(x_2 - x_1 - \xi)^2 + \eta_0^2\right]^{3/2}}, \tag{6}$$

and

$$Y = \frac{\rho U_2}{4\pi} \int_{L_1} (2U_2 - U_1) S_1'(x_1) \int_{L_2} \frac{\eta_0 S_2'(x_2)\,\mathrm{dx_2\,dx_1}}{\left[(x_2 - x_1 - \xi)^2 + \eta_0^2\right]^{3/2}}. \tag{7}$$

We assume a cross-sectional area distribution of parabolic form

$$S_j(x_j) = S_j(0)\left(1 - 4x_j^2/L_j^2\right), \tag{8}$$

where $S_j(0)$ is the mid-body cross-sectional area of the jth body, and $S_j' \equiv \mathrm{d}S_j(x)/\mathrm{d}x$.

$$\begin{aligned} F_X &\equiv X/\left[\rho U_2^2 L_1^2 (S_1/L_1^2)(S_2/L_2^2)\right]; \\ F_Y &\equiv Y/\left[\rho U_2^2 L_1^2 (S_1/L_1^2)(S_2/L_2^2)\right]. \end{aligned} \tag{9}$$

Note that the shape given in Eq. (8) is a reasonable assumption for many marine animals, such as dolphins, as well as submarines and missiles.

3 Higher order approximation and small separation distances

We now obtain a solution that includes smaller lateral separation distances, i.e. $O(\epsilon)$. Since the lateral separation distances become $O(\epsilon)$, the assumption of a constant lateral separation distance between the body contours becomes inaccurate, and the need for a more accurate definition of the actual lateral separation distance $O(\epsilon)$ arises, such that the separation distances between the borders of the two bodies are taken instead of the constant centrelines separation distance.

3.1 Exact lateral separation distance

The exact value of the separation distance between the laterally closest points on the bodies is now $\eta = \eta(x_1, x_2)$, which is a function of the geometry of the two bodies. In general, such an approximation to the exact lateral separation distance can be made when the flow field is considered symmetric in the y–z plane, and the centrelines of the two bodies are in the plane $z_1 = z_2 = z = 0$. To this end, we use the simple cross-sectional area of the form given in Eq. (8). Extracting the radius r_j from the relation

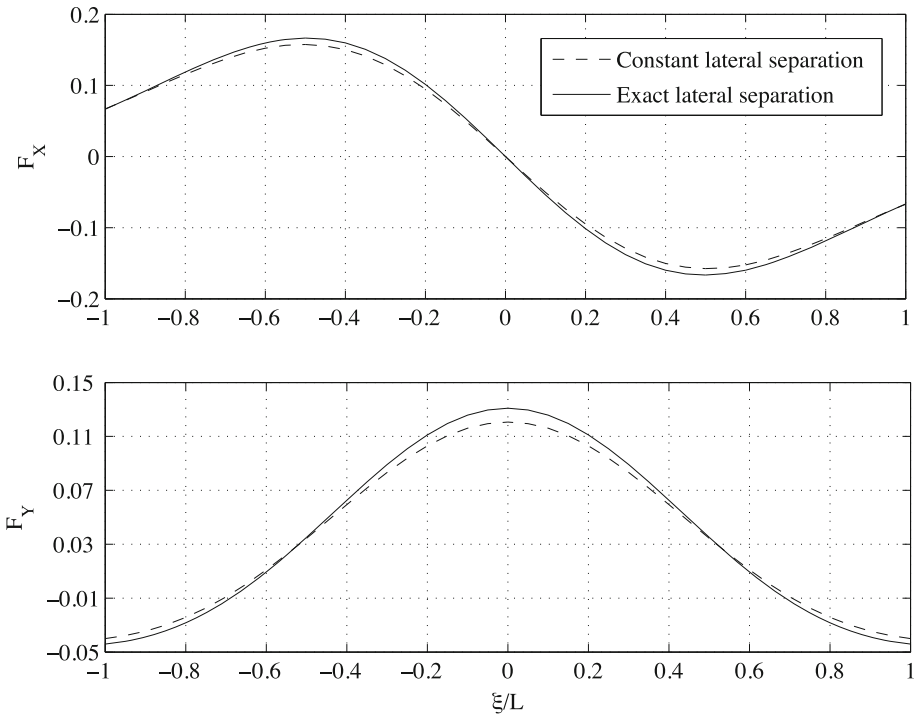

Fig. 2 Nondimensional longitudinal (*top*) and lateral (*bottom*) forces F_X and F_Y on body 1 vs. location of body 2 to body 1 ξ/L with constant $\eta_0 = L/2$ and exact η; when $\xi/L = 1$ the tip of body 1 and the toe of body 2 are at the same longitudinal location

$S_j(x_j) = \pi r_j^2$ and substituting into Eq. (8) yields

$$r_j(x_j) = \sqrt{S_j(0)\left(1 - 4x_j^2/L_j^2\right)/\pi}, \tag{10}$$

The general form of the separation distance $\eta(x_j)$ is given by

$$\eta(x_1, x_2) = \eta_0 - \sum_{j=1,2} r_j(x_j), \tag{11}$$

where η_0 is the constant separation distance between the parallel paths of the two bodies, and $\sum_{j=1,2} r_j(x_j)$ equals the total radii to be subtracted. Substituting Eq. (10) into Eq. (11) yields

$$\eta = \eta_0 - \left[\sqrt{S_1(0)\left(1 - 4x_1^2/L_1^2\right)/\pi} + \sqrt{S_2(0)\left(1 - 4x_2^2/L_2^2\right)/\pi}\right]. \tag{12}$$

The calculations made here are for constant and (normalised) equal velocities $U_1 = U_2 = 1$; the forces are calculated at different but fixed separation distances. Figure 2 shows the longitudinal and the lateral forces calculated first using a constant separation distance η_0, and compared with the forces calculated using the exact η, as a function of the longitudinal separation distance ξ; η_0 in Eqs. (6) and (7) is replaced by η, and then substituted in (9). Note that The body length $L = 1$, and the separation distance η_0 is taken as half the body length, and the two bodies are identical with slenderness ratio 1 : 6 (i.e. $d = 1/6$ and $S_j(0) = \pi d^2/4$). The deviation is perceived mostly in the peak regions, in which the relative longitudinal distance is either half-body length (top subplot), or zero- or full-body length (bottom), for the longitudinal and lateral forces, respectively; and if vice versa a zero deviation is noticed.

Figure 3 shows the peak longitudinal and lateral forces as a function of the separation distance (assumed to be constant in the previous sections), compared with the longitudinal and the lateral forces calculated using the exact separation distance η (solid curve). The constant separation distance η_0 (dashed curve) is taken with a range of half-body to full-body length, $0.5 < \eta_0/L < 1$. Figure 3 shows a monotonic increase of the deviation between the two curves as the separation distance decreases. The increased deviation for a smaller separation distance is relatively more significant for the lateral forces, reaching 10 % compared to 5 % for the longitudinal forces.

For small separation distances $\eta = O(\epsilon)$, it is insufficient to consider the exact separation distance alone. The neglected higher order forces become significant compared to the first-order approximation. Therefore, there is a need to include the next terms of the perturbation velocity potential, terms that are at least of the same order of η. These higher order effects are investigated in the following section.

3.2 Higher order solution

Defining λ as the exact distance between two points on the surfaces of the two bodies we can write

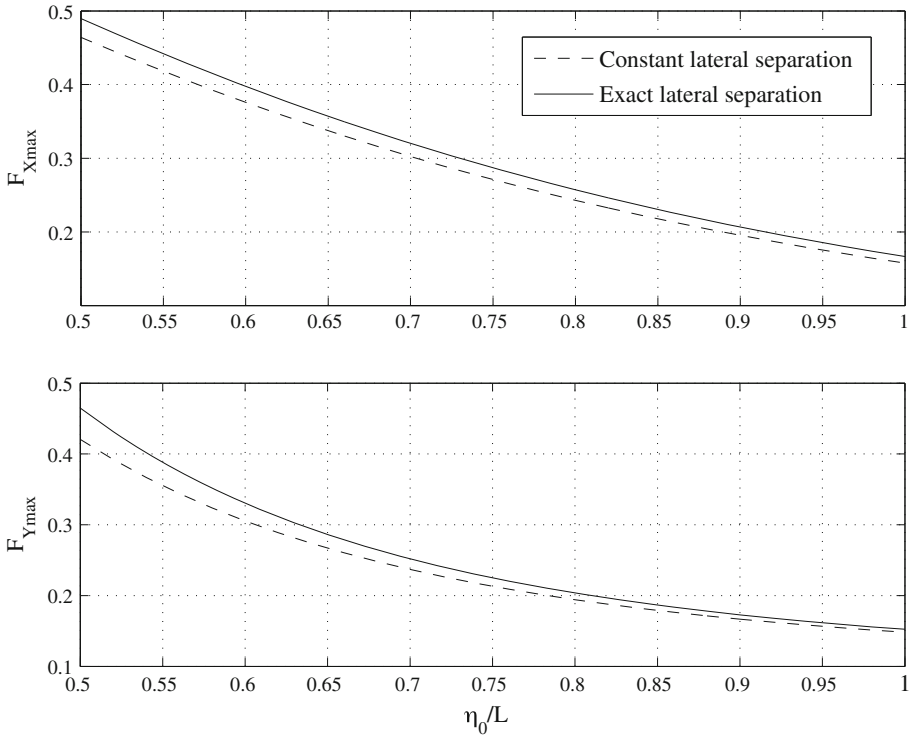

Fig. 3 Nondimensional peak longitudinal (*top*) and lateral (*bottom*) forces $F_{X\max}$ and $F_{Y\max}$ on a stationary body vs. the normalised lateral separation η/L from a passing body with $0.5<\eta_0/L<1$, and $\xi/L=0.5$ (*top*) or $\xi/L=0$ (*bottom*)

$$\lambda=\left\{\xi^2+\left[\eta_0-\frac{1}{2}(\epsilon_1 L_1+\epsilon_2 L_2)\right]^2\right\}^{1/2}, \tag{13}$$

For slender bodies $\epsilon_j \ll 1$, and again considering them identical, $\epsilon_1=\epsilon_2=\epsilon$ and $L_1=L_2=L$, we find that

$$\lambda^2=\xi^2+\eta_0^2-2\eta_0\epsilon L+\frac{\epsilon^2 L^2}{2} \tag{14}$$

For $\eta_0\sim O(1)$, the second term—the leading order—of the right hand of Eq. (14) is $O(1)$, the third is $O(\epsilon)$, and the fourth is $O(\epsilon^2)$. However, for the case $\eta_0\sim O(\epsilon)$, the second, third and fourth terms on the right-hand side of (14) all become of $O(\epsilon^2)$, which means that for this case all second-order terms should be considered.

Following [36], for the longitudinal motion, the potential due to the body disturbance is of the form,

$$\Phi=U_i\phi_i. \tag{15}$$

For $r\ll L$, the three-dimensional velocity potential in the outer region can be expanded about the other body, in the form

$$\phi_2(x_2,y_2,z_2)=\phi(x_2,-\eta,0)+(y+\eta)\left(\frac{\partial\phi}{\partial y}\right)_{y=-\eta}+\frac{(y+\eta)^2}{2}\left(\frac{\partial^2\phi}{\partial y^2}\right)_{y=-\eta}+\ldots \tag{16}$$

Using the method of matched asymptotic expansions we shall find a solution to the longitudinal motion problem. The inner solution Φ_1 is governed by the two-dimensional Laplace equation and the no penetration boundary condition. The outer solution, φ_1, is governed by the three-dimensional Laplace equation and by the condition at infinity where the potential vanishes. These two solutions can be matched in an overlap region $\epsilon^2 L\ll r\ll$. This leads to,

$$\varphi_1\simeq\Phi_1,\quad \epsilon^2 L\ll r\ll L, \tag{17}$$

where based on [36], pp. 336, and a Taylor expansion:

$$\Phi_1\simeq-\frac{S'}{2\pi}\left[\ln\left(\frac{r}{L}\right)+\frac{L}{r}-\frac{L^2}{r^2}\right]+f(x),\qquad \text{for } r>>\epsilon^2 L. \tag{18}$$

Combining (17) and (18), we get the inner condition for φ_1 in the form

$$\varphi_1\simeq-\frac{S'}{2\pi}\left[\ln\left(\frac{r}{L}\right)+\frac{L}{r}-\frac{L^2}{r^2}\right]+f(x),\ \text{for } r\ll L, \tag{19}$$

where $f(x)$ is found by the matching requirements

$$f(x)=\frac{1}{4\pi}\int_{-L/2}^{x}S''(\xi)\ln[2(x-\xi)/L]\mathrm{d}\xi-\frac{1}{4\pi}\int_{x}^{L/2}S''(\xi)\ln[2(\xi-x)/L]\mathrm{d}\xi. \tag{20}$$

The appropriate outer solution is a distribution of multipoles, along the body axis. Using the three-dimensional

potential source and its derivatives, and distributing them along the body axis gives

$$\varphi_1(x,r) = \frac{1}{4\pi}\int_L \frac{S'(\xi)\mathrm{d}\xi}{\left[(x-\xi)^2+r^2\right]^{1/2}} + \frac{r_0}{4\pi}\int_L \frac{S'(\xi)r\mathrm{d}\xi}{\left[(x-\xi)^2+r^2\right]^{3/2}} + \frac{r_0^2}{4\pi}\int_L \left\{\frac{3}{2}\frac{S'(\xi)r^2}{\left[(x-\xi)^2+r^2\right]^{5/2}} - \frac{1}{2}\frac{S'(\xi)}{\left[(x-\xi)^2+r^2\right]^{3/2}}\right\}\mathrm{d}\xi, \tag{21}$$

where r_0 is the radius of the mid-body cross-sectional area.

Expanding the boundary conditions and substituting $g \equiv (x_2 - x)^2 - \eta^2$ the cross-flow becomes

$$V(x_2) = \frac{U_2\eta}{4\pi}\int_{L_j} S_2'(x)\left(\frac{1}{g^{3/2}} + \frac{3}{2}\frac{\eta^2}{g^{5/2}}\right)\mathrm{dx} + \mathrm{O}(\epsilon^3). \tag{22}$$

The total lateral forces on body 1 are given by

$$Y = \rho\int_{L_1}[\mathrm{D}(\mathrm{VA}_1) + \mathrm{S}_1\mathrm{D}(\mathrm{V})]\mathrm{dx}_1, \tag{23}$$

where $D = \partial/\partial t - U_j\partial/\partial x_j$ is in reference frames 1 and 2, respectively (see figure 1); and ρA_1 is the added mass per unit length. For bodies of revolution $A_1 \equiv S_1$ (see [22]). Substituting (22) into Eq. (23) and taking into consideration the exact separation distance effect, the following second-order approximation of the lateral forces is finally obtained

$$Y(\xi) = \frac{\rho U_2}{4\pi}\int_{L_1}\Big\{(2U_2 - U_1)S_1'(x_1) \times \int_{L_2}\frac{\eta(x_1,x_2)S_2'(x_2)}{\left[(x_2-x_1-\xi)^2+\eta^2(x_1,x_2)\right]^{3/2}}\mathrm{dx}_2\Big\}\mathrm{dx}_1 + \frac{3}{2}\frac{\rho U_2}{4\pi}\int_{L_1}\Big\{(2U_2 - U_1)S_1'(x_1) \times \int_{L_2}\frac{\eta^3(x_1,x_2)S_2'(x_2)}{\left[(x_2-x_1-\xi)^2+\eta^2(x_1,x_2)\right]^{5/2}}\mathrm{dx}_2\Big\}\mathrm{dx}_1 \tag{24}$$

Note that the second-order approximation for the yawing moments can be derived directly from Eq. (24). The higher order approximation terms of the longitudinal forces are negligible compared to the leading-order term (the velocity potential in the longitudinal case does not contain the separation distance term η in the numerator). According to the slender body theory, the body has an infinite length relative to its cross-sectional dimensions, and the fluid velocity in the longitudinal direction is assumed to be constant to first order.

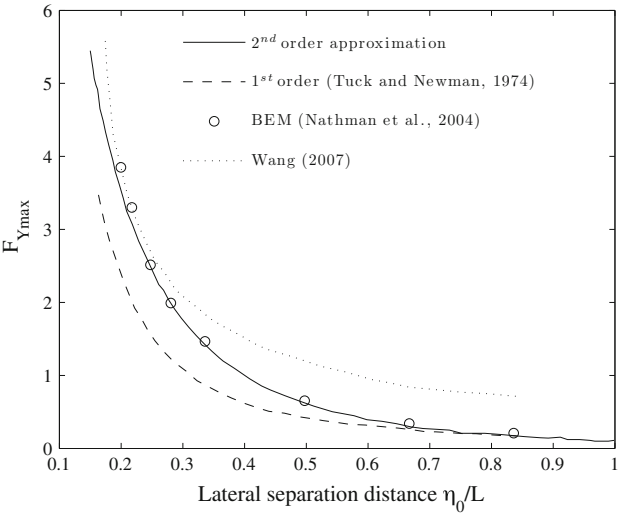

Fig. 4 Nondimensional peak lateral forces $F_Y max$ on body 1 as a function of its normalised lateral separation η_0/L, with $\xi = 0$, $\epsilon = 0.1$, and $\epsilon < \eta_0/L < 1$

Figure 4 presents calculations of the nondimensional peak lateral forces acting on body 1 as function of the lateral separation distance. The second-order effects are considered and compared with the first-order approximation, and other solutions found in the literature. The solid curve represents the current second-order approximation; the dashed curve represents the first-order approximation solution (the same solution is also given by Tuck [22]); the open circles are numerical results using a boundary element method [35], which was originally presented in [34]; and the dotted curve is the analytical solution of two slender bodies moving in very close proximity by Wang [34]. A range of separation distances $\eta_0/L = (0.1, 1)$ is considered. Figure 4 shows that while the first-order solution is in good agreement with the numerical calculations only at relatively large separation distances $\eta_0/L > 0.7$, and the solution by Wang [34] is in good agreement with the numerical calculations only at relatively small lateral separation distances $\eta_0/L < 0.3$, our proposed second order approximation gives a satisfactory agreement at the entire range of separation distances $\epsilon < \eta_0/L < 1$.

Following [9], calculations were made for two ships moving in parallel at equal velocities, at various stagger distances. The experimental results of the interaction effects between the two ships were reported by Newton [2]. The first ship (Ship A) was the battleship King George V, of length 740 feet, beam 103 feet, draft 29.3 feet, and displacement 36,890 tons. The second ship (Ship B) was the R.F.A. Olna, of length 567 feet, beam 70 feet, draft 30 feet, and displacement 23,570 tons. The two mid–body sectional areas were 3050 and 2075 square feet, respectively. Their sectional area distributions departed only

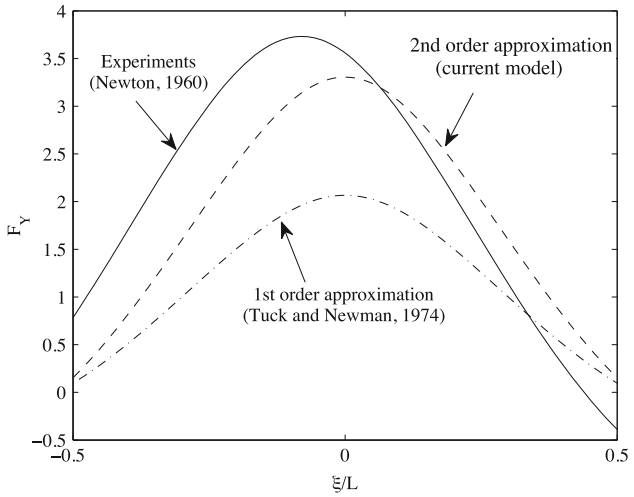

Fig. 5 Lateral forces on two ships, $F_Y = Y_{\text{Newton}}/(\text{tons}/10(\text{knot})^2)$ (the original figure was given by Newton [2])

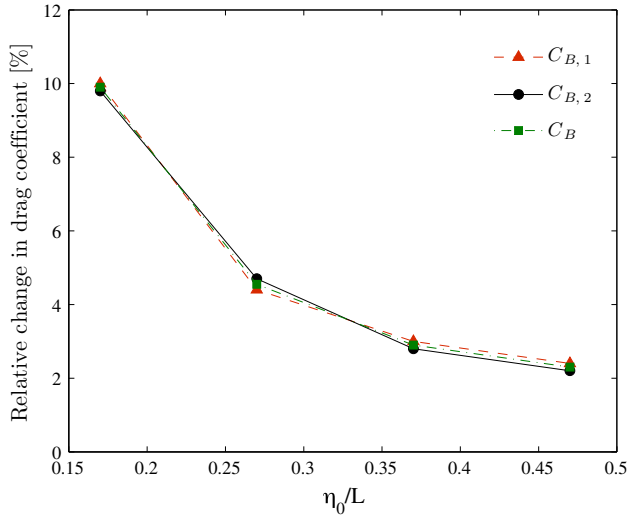

Fig. 6 Individual and combined drag coefficients for two parallel bodies, with $\xi = 0$ and $0.17 < \eta_0/L < 0.47$. Based on figure 6 of [38]

slightly from parabolic curves, and Ship A was slightly fuller, so that these departures should cancel out.

The results of the lateral forces obtained by Wang [9] agree with those obtained by Tuck [22] and are in qualitative agreement with experiments, however, their theoretical results are 30–40 % lower than the experiments. Applying the second-order approximation solution presented in this paper results in improved agreement with experiments as shown in Fig. 5. There are still some discrepancies, which can be explained as follows. The peak interaction force in the experiments is still larger than our prediction and is somewhat earlier than our prediction. The reasons for this discrepancy are: first and most crucial, free surface effects [23], or the lifting-body effect due to vortex sheet shed from the stern [25], which are not included in our analysis of submerged bodies and boundary layer effects change the actual point of closest approach in the longitudinal direction; second, the ship tested did not have a fore-aft symmetry.

4 Summation

The forces and moments on a body immersed in incompressible fluid resulting from the hydrodynamic interactions induced by the movement of a second body are strongly dependent on the lateral separation distance. We calculate the forces on two submerged bodies moving together at different longitudinal distances between bows, building up a quasi-steady solution for the forces during an overtaking manoeuvre.

The results shown in Fig. 3 provide a conservative estimate for the peak forces acting on body 1 due to the movement of body 2. The lateral forces acting on body 1 for the case where the two bodies move at equal velocities, are half the forces acting on body 1 for the case it was stationary [34, 42]. Obviously, the forces acting on the two bodies would become larger if they were moving in opposite directions (e.g. see [34] or [42]).

The contribution of the additional forces due to considering the exact lateral separation distance was found to be small even for relatively small lateral separation distances, and negligible for large separation distances. The additional lateral forces are the largest at zero longitudinal offset.

Applying the second-order approximation provides much better qualitative and quantitative agreement with the experimental measurements carried out by Newton, as well as with the numerical results of the boundary element method presented by Newton [34], solving previous discrepancies. Carrying out even higher order potential approximations is probably not very useful, as the neglected viscous effects become more important.

Acknowledgments The research is based on an M.Sc. thesis submitted by U.K. to the Graduate School of the Technion-Israel Institute of Technology, 2005.

Note added in proof The analyses carried out in the previous sections neglected viscosity effects. As mentioned above a recent study [37, 38], which appeared while this paper was under initial review, examined, among others, the impact of spacing between slender bodies on the viscous drag. Following [37], we define

$$C_{B,j} = \frac{C_{D(B,j)} - C_{D(s)}}{C_{D(s)}}, \quad \text{for } j = 1, 2$$
$$C_B = \frac{1}{2}\sum_{j=1}^{2} C_{B,j}, \tag{25}$$

where $C_{B,j}$ is the difference of the drag of body j relative to a single hull drag $C_{D(s)}$, and C_B is the combined (averaged) drag. For the case

presented in figure 4 with zero longitudinal offset ($\xi = 0$) the hulls of the two bodies experience an equal drag increase associated with the increase in skin friction drag, as presented in Fig. 6 (also see figure 6 of [38]). As the lateral separation distance decreases to $\epsilon\,(=1/6)$, the accelerated flow increases, resulting in a 10 % drag increase compared to less that 2 % at $\eta_0/L \simeq 0.47$ (see Fig. 6), as also suggested by Hoerner [39], Hucho and Ahmed [40], and Molland and Utama [41].

References

1. Taylor GI (1928) The force acting on a body placed in a curved and converging stream fluid. Proc R Soc Lond A 120:260
2. Newton RN (1960) Some notes on interaction effects between ships close aboard in deep water. In: Proceedings of first symposium on ship maneuverability, DTMB Report 1461, Washington, D.C., pp 1–24 (1960)
3. Silverstein BL (1957) Linearized theory of the interaction of ships. Institute of Engineering Research, University of California, Berkeley, Calif, Tech. Rep., Series 82, Issue 3
4. Collatz G (1963) Potential theoretische Unter suchnung der hydrodynamicschen Wechselwirkung zweier Schiffskorper. Jahrbuch Schiffsbautechnischen Gesellschaft 57:281–329
5. Dand IW (1974) Some aspects of maneuvering in collision situation in shallow water. In: Proceedings of tenth symposium on naval hydrodynamics, Cambridge MA. Office of Naval Research, Washington, pp 261–275 (1974)
6. Tuck EO (1978) Hydrodynamic problems of ships in restricted waters. Annu Rev Fluid Mech 10:33–44
7. Newman JN (1965) The force and moment on a slender body of revolution moving near a wall. Naval Ship R&D Centre Rep. 2127
8. Newman JN (1972) Some theories for ship maneuvering. International symposium on directional stability and control of bodies moving in water, London, pp 34–42
9. Wang S (1974) Forces and moment on a moored vessel. In: Tenth symposium on naval hydrodynamics, Cambridge MA. Office of Naval Research, Washington, pp 62–69
10. Wang QX (1992) Analysis of slender bodies of revolution with curved-ground effect and waving-water effect. Fluid Dyn Res 9:235–254
11. Milne-Thomson LM (1968) Theoretical hydrodynamics, 5th edn. The Macmillan Press LTD, pp XVI, XVII, 528–530 (1968)
12. Munk MM (1924) The aerodynamic forces on airship hulls. NACA Rep. 184
13. Lighthill MJ (1954) General theory of high speed aerodynamics. In: High-speed aerodynamics and jet propulsion, vol 6. Princeton Univ. Press, Princeton, pp sect. E, pp 462–477
14. Cole JD, Messiter AF (1957) Expansion procedures and similarity laws for transonic flow; I. slender bodies at zero incidence. Z Angew Math Physik 88:1–25
15. Dyke MV (1959) Second-order theory-axisymmetric flow, Tech. Rep. NASA R-47
16. Barrows TM (1971) Progress on the ram-wing concept, with emphasis on lateral dynamics, Tech. rep., US Dept. Trans. Rep
17. Tuck EO (1975) Matching problems involving flow through small holes. Adv Appl Mech 15:89–158
18. Norrbin NH (1974) Bank effects on a ship moving through a short dredged channel. In: Tenth symposium on naval hydrodynamics, Cambridge MA. Office of Naval Research, Washington, pp 71–88 (1974)
19. Newman JN (1970) Applications of slender-body theory in ship hydrodynamics. Annu Rev Fluid Mech 2:67–94
20. Ogilvie TF (1974) Slender-ship theory. Workshop on slender-body theory, part 1: free surface effects, Tech. rep., University of Michigan, Department of Naval Architecture and Marine Engineering, p 13
21. Ogilvie TF (1977) Singular perturbation problems in ship hydrodynamics. Adv Appl Mech 17:92–187
22. Tuck EO, Newman JN (1974) Hydrodynamic interactions between ships. In: Cooper R, Doroff S (eds) In: Tenth symposium on naval hydrodynamics. U.S. Government Printing Office, Washington, pp 35–70
23. Yeung RW (1978) On the interactions of slender ships in shallow water. J Fluid Mech 85:143–159
24. Yeung RW, Tan WT (1980) Hydrodynamic interactions of ships with fixed obstacles. J Ship Res 24:50–59
25. Kijima K (1979) Hydrodynamic interactions between two lifting bodies. Japan Soc Naval Archit 58:187–197
26. Kijima K, Furukawa Y, Qing H (1991) The interaction effects between two ships in the proximity of bank wall. The Japan Society of Naval Architects and Ocean Engineers, vol 81, pp 101–112
27. Faltinsen OM, Newman JN, Vinje T (1995) Nonlinear-wave loads on a slender vertical cylinder. J Fluid Mech 289:179–198
28. Fontaine E, Faltinsen OM, Cointe R (2000) New insight into the generation of ship bow waves. J Fluid Mech 421:15–38
29. Becker LE, Koehler SA, Stone HA (2003) On self-propulsion of micro-machines at low reynolds number: Purcells three-link swimmer. J Fluid Mech 490:15–35
30. Chen XN, Sharma SD, Stuntz N (2003) Zero wave resistance for ships moving in shallow channels at supercritical speeds. Part 2. Improved theory and model experiment. J Fluid Mech 478:111–124
31. Lighthill MJ (1960) Note on the swimming of slender fish. J Fluid Mech 9:305
32. Newman JN, Wu TY (1973) A generalized slender-body theory for fish-like form. J Fluid Mech 57:673–697
33. Weihs D (2004) Dolphin drafting hydrodynamics. J Biol 3:1–16
34. Wang QX (2007) An analytical solution for two slender bodies of revolution translating in very close proximity. J Fluid Mech 582:223–251
35. Nathman JK, Matarrese M (2004) Hybrid grid (structured and unstructured) calculations with a potentialbased panel method. In: AIAA Paper 2004-4836
36. Newman JN (1977) Marine hydrodynamics, 3rd edn. The MIT Press, Cambridge
37. Rattanasiri P, Wilson PA, Phillips AB (2014) Numerical investigation of a fleet of towed AUVs. Ocean Eng 80C:25–35. doi:10.1016/j.oceaneng.2014.02.001
38. Rattanasiri P, Wilson PA, Phillips AB (2012) Numerical Investigation of the influence of propeller to the interference drag of twin prolate spheroids at various longitudinal offsets and transverse separations. In: USYS'12: 4th international conference on underwater system technology, Southampton
39. Hoerner SF (1965) Fluid-dynamic drag: practical information on aerodynamic drag and hydrodynamic resistance. Published by the author
40. Hucho WH, Ahmed SR (1998) Aerodynamics of road vehicles: from fluid mechanics to vehicle engineering, 4th edn. The Society of Automative Engineers, Warrendale
41. Molland AF, Utama IKA (2002) Experimental and numerical investigations of a pair of ellipsoids in close proximity. In: Proceedings of the Institute of Mechanical Engineers, Part M: Journal of Engineering for Maritime Environment (2002)
42. Kadri U (2005) The flow field and forces on two slender bodies moving in close proximity, M.Sc. Thesis, Technion Libraries, Israel Institute of Technology, Haifa